Digital Orthophoto Production Using Close-Range Photographs for High Curved Objects

Fanar Mansour Abed
Assistant Lecturer
College of Engineering- University of Baghdad
fanar.mansou@coeng.uobaghdad.edu.iq

ABSTRACT

Orthophoto provides a significant alternative capability for the presentation of architectural or archaeological applications. Although orthophoto production from airphotography of high or lower altitudes is considered to be typical, the close range applications for the large-scale survey of statue or art masterpiece or any kind of monuments still contain a lot of interesting issues to be investigated.

In this paper a test was carried out for the production of large scale orthophoto of highly curved surface, using a statue constructed of some kind of stones. In this test we use stereo photographs to produce the orthophoto in stead of single photo and DTM, by applying the DLT mathematical relationship as base formula in differential rectification process. The possibilities and the restrictions of the used programs for the extraction of digital surface model & orthophoto production were investigated. The accuracy of the adjusted images using the digital differential rectification package, are checked using 3 check points and the RMSE was computed in 3-dimensions. Conclusions for usefulness and reliability of this test for such special applications were derived.

Key words: photogrammetry, close-range, orthophoto, DLT

انتاج الصور ذات الاسقاط العمودي باستخدام تقنية المسح التصويري ذو المدى القريب لاجسام ذات سطوح معقدة

فنار منصور عبد
مدرس مساعد
كلية الهندسة- جامعة بغداد

الخلاصـــة

ان الصور ذات الاسقاط العمودي تعتبر احد قابليات الوصف الدقيقة والمهمة في الكثير من التطبيقات وخاصة المعمارية وتطبيقات علم الاثار. فعلى الرغم من ان الصور ذات الاسقاط العمودي المستحصلة عن طريق المسح التصويري الجوي سواء كانت الصور المستخدمة ملتقطة من ارتفاعات عالية او واطئة يمكن ان نعتبرها صور مثالية ، الا ان تطبيقات استحصال الصور ذات الاسقاط العمودي من صور ارضية ذات المدى القريب وبمقياس كبير والملتقطة لاهداف تمثل اي نوع من انواع التماثيل او التحف الفنية (كالقطع الاثارية مثلا) ، لا تزال تحتاج الى الكثير من التجارب والمحاولات الخاصة بمسالة دقة مواقع النقاط على هذه الاهداف. ولهذه الاسباب تم اعداد هذا البحث والمتمثل بانتاج صورة ارضية ذات اسقاط عمودي وبمقياس كبير لهدف يتكون من نوع من انواع التماثيل والمصنوع من احد انواع الاحجار والذي يتميز بسطحه الحاوي على

الكثير من المعالم الحادة والكثيرة الانحناءات وذلك من خلال التقاط صورتين للهدف (يمنى ويسرى) من على بعد مناسب للحصول على منطقة تداخل بين الصورتين من اجل الحصول على البعد الثالث. ان الية العمل في هذا البحث اعتمدت على استخدام زوج الصور في انتاج الصورة ذات الاسقاط العمودي بدلا من الطريقة الشائعة والمتمثلة في استخدام صورة واحدة وDTM. حيث تم العمل في هذا البحث من خلال تطبيق الموديل الرياضي للتقويم التفاضلي بالاعتماد على التحويل الخطي المباشر (DLT).

الكلمات الرئيسية: المسح التصويري, المدى القريب, الصور ذات الاسقاط العمودي, معادلات التحويل الخطي

1. INTRODUCTION

Orthophotography is a powerful tool for aerial photogrammetric applications, already tested with excellent results, cost effective and extremely flexible in its digital version ,loannidis, et al., 2003. In terrestrial and especially in close-range applications digital rectification and the development of mathematically developable surfaces are mostly applied when stereoscopic photogrammetric procedures are used. In architectural and especially in archaeological applications, however, one is very often faced with surfaces, one which these procedures cannot be applied, while at the same time the desired result is an image ,**Hemmleb, 2002**. In this case the production of an orthophotography seems to be the only solution, capable of providing reliable and accurate results.

The idea for carrying out this test described in this article was the investigation of the undisputed possibilities presented and the problems which arise when applying orthophoto techniques in difficult cases of geometric documentation of monuments and any other applications in archaeological field. It goes without saying that this particular product is extremely valuable, especially as coverage of a Spatial Information System. The investigation in this test concerns the possibilities of producing satisfactory results for close-range archaeological applications on highly curved objects, using a package of digital differential rectification that is based on Direct Linear Transformation (DLT) equations.

2. PROCEDURES OF THE WORK

2.1 Field Work

The used target was some kind of statues that have been chosen because of its high curved surface with tiny details having 15 marked points on it, to be the control points, see **Fig.1** These points were circles with diameter of 0.5mm, have been lately computed very accurately in 3-dimensions using T2 theodolite with its accessories and steel tape. These points includes 3 check points that used later to find the RMSE.

The structure of the field work was:-

- Creating a base line (AB between two very accurate ground points A & B) far away from the target about 1.735m vertical from the middle.
- Observed the points on the target from stations A&B and record both horizontal and vertical angles, using sets for high accuracy.

- Compute the X&Y ground coordinates for the 15 points using intersection I and also compute the height (Z) of these points by sum the vertical distance to the height of instrument, see **Table 1**.
- Taking the left and right photos to the target from different stations (C & D), see **Fig.2** using a non metric digital camera (Fujitech, 5.1 megapixels) mounted on a level tript in front of the target. The specifications of the digital camera are listed in **Table 2**.

2.2 Geometric Correction of Digital Images

Geometric errors and displacements in digital images are caused by the characteristics of the acquisition process and the geometric characteristics of the object being imaged. These geometric corrections consist of two steps:

1. Model the geometric errors in the image by an appropriate mathematical formula. This formula can be either:
   - A rigorous mathematical model describing the relationship between the image and the ground, in our case Direct Linear Transformation (DLT) formula have been used which represented by the differential rectification process.
   - An empirical relationship such as 1^{st} through n^{th} order polynomial equations which do not model the true geometric relationships between the image and the ground, this is represented by the polynomial rectification process.
2. Resample the image by computing a new image with the pixels in known positions and known dimensions, such that the image will represent the correct geometry of the object. Resampling produces a new data set from an existing old one. It usually involves both geometric and intensity domains. Resampling comprises two basic stages :
   - Calculation of the new pixel locations.
   - Interpolation of the corresponding intensity levels from the neighboring old pixels.

2.2.1 Differential rectification

In the case of digital differential rectification, each pixel is separately transferred from the original image to the resulting image using the indirect approach (from ground to image). A Digital Train Model (DTM) is needed to correct for relief displacements in the image. It is assumed that the DTM is stored in the same format as the digital image, which in this case expresses elevations instead of densities. In general case, digital differential rectification is done using one image and existing DTM in the following manner:

Measuring the digital image coordinates (column, row) for control points where corresponding ground control coordinates of these measured image coordinates are input and used to solve the DLT formula. A least squares solution is employed to include any number of redundant measurements and assess the quality of the solution matrix. The DEM is then interpolated to produce coordinated ground point locations at required intervals. Rectified image coordinates corresponding to these ground point locations are then computed using the inverse condition of DLT. The final step is to compute the gray value for each pixel by interpolation using one of the resampling methods. The density is stored at the X,Y location of digital orthophoto.

In this paper we did not use the DTM for our study spot; therefore we used a method for digital orthophoto production which depends on the use of stereo pair images instead of the use of one image and DTM.

2.2.2 Direct linear transformation (DLT)

Among the approaches particularly suitable for non-metric photography is the Direct Linear Transformation (DLT) approach. The solution is based on the concept of direct transformation from image coordinates into object-space coordinates, thus by passing the traditional intermediate step of transforming image coordinates from machine system to photo system, ,**Sharki, 2002**. The method is based on the following pairs of equations:

$$x + \frac{L_1X + L_2Y + L_3Z + L_4}{L_9X + L_{10}Y + L_{11}Z + 1} = 0 \quad \text{…. (1)}$$

$$y + \frac{L_5X + L_6Y + L_7Z + L_8}{L_9X + L_{10}Y + L_{11}Z + 1} = 0 \quad \text{…. (2)}$$

Where:

$x \,\&\, y$ are the measured digital image coordinates
$X, Y \,\&\, Z$ are the object space coordinates
L_1 to L_{11} are eleven unknown constants

If we added for Eqs. (1) and (2) the errors due to the optical and de-centering distortion, they become:

$$(x + \Delta x) + \frac{L_1X + L_2Y + L_3Z + L_4}{L_9X + L_{10}Y + L_{11}Z + 1} = 0 \quad \text{…. (3)}$$

$$(y + \Delta y) + \frac{L_5X + L_6Y + L_7Z + L_8}{L_9X + L_{10}Y + L_{11}Z + 1} = 0 \quad \text{…. (4)}$$

Where:

$$\Delta x = x(L_{12}r^2 + L_{13}r^4 + L_{14}r^6) + L_{15}(r^2 + 2x^2) + 2L_{16}yx \quad \text{.... (5)}$$

$$\Delta y = y(L_{12}r^2 + L_{13}r^4 + L_{14}r^6) + 2L_{15}xy + L_{16}(r^2 + 2y^2) \quad \text{.... (6)}$$

$$r^2 = x^2 + y^2 \quad \text{…. (7)}$$

L_{12} to L_{14} are the coefficients of optical distortion
$L_{15} \,\&\, L_{16}$ are the coefficients of de-centering distortion

By substituting the values of $\Delta x \,\&\, \Delta y$ to Eqs. (3) and (4), simplified and re-arranged, we obtain:

$$x = L_1X + L_2Y + L_3Z + L_4 - xL_9X - xL_{10}Y - xL_{11}Z - xL_{12}r^2R - xL_{13}r^4R - xL_{14}r^6R - \left(L_{15}\left(r^2 + 2x^2\right)\right)R - 2L_{16}xyR \quad \text{.... (8)}$$

$$y = L_5X + L_6Y + L_7Z + L_8 - yL_9X - yL_{10}Y - yL_{11}Z - yL_{12}r^2R - yL_{13}r^4R - yL_{14}r^6R - 2L_{15}xyR - L_{16}\left(r^2 + 2y^2\right)R \quad \text{.... (9)}$$

Where:

$$R = L_9X + L_{10}Y + L_{11}Z + 1 \quad \text{.... (10)}$$

To obtain the DLT parameters using the least square method, we have to solve Eqs. (8) and (9) in matrix form.
In this test we used the 15 ground points to solve the 16 parameters, so, each point gives 2 equations and the total number of equations will be 30 equations. At first we measured the digital coordinates of these points on both photos , see **Table 3.** then by solving these equations using L.S. we gain the parameters listed below:

LEFT PHOTO:-

$L_1 = -0.00300897657871246$
$L_2 = 0.0892554074525833$
$L_3 = -0.205902293324471$
$L_4 = 1.0034114074707$
$L_5 = 0.137721985578537$
$L_6 = -0.135213151574135$
$L_7 = -0.106498301029205$
$L_8 = -8.93060302734375$
$L_9 = -0.000532188263605349$
$L_{10} = -4.21748918597586E-005$
$L_{11} = -0.00145815122232307$
$L_{12} = -8.71862795293055E-007$
$L_{13} = 2.88788825887837E-013$
$L_{14} = -3.25629802096636E-020$
$L_{15} = -1.093368337024E-005$
$L_{16} = -4.72695683129132E-006$

RIGHT PHOTO:-

$L_1 = -0.2379578637332$
$L_2 = 0.071085112169385$
$L_3 = -0.201956253498793$
$L_4 = 2.17296390533447$
$L_5 = -0.147681787610054$
$L_6 = 0.0615520495921373$
$L_7 = -0.129928223788738$
$L_8 = 1.36469879150391$
$L_9 = -0.00120378778683516$
$L_{10} = 0.000344896406204498$
$L_{11} = -0.000825379638627055$
$L_{12} = -1.56502965609207E-006$
$L_{13} = 6.52899424723684E-013$
$L_{14} = -9.84681762699648E-020$
$L_{15} = 0.000101436824479606$
$L_{16} = 5.93337208556477E-005$

2.2.3 Preparation of (TIN) for the study spot

Most of the previous works in the field of digital orthorectification depend upon the standard DTM, ,**Mikhail et al., 2001**. In this work, a method of preparing Triangulated Irregular Network (TIN) is presented. This method is done through two steps:

The first step: is the matching between the two images, using manual matching in this case, by selecting 35 dispersed points on the target and record the digital coordinates of these points for both left & right photos, the distribution of these points on the target is shown in **Fig.3** and the digital coordinates (column,row) of these points are listed in **Table 4**.

The second step: is computing the ground coordinates of these matched points, and this is done using the following equations:

$$(L_1 + x_i L_9)X_i + (L_2 + x_i L_{10})Y_i + (L_3 + x_i L_{11})Z_i + x_i + L_4 = 0 \quad \text{.... (11)}$$

$$(L_5 + y_i L_9)X_i + (L_6 + y_i L_{10})Y_i + (L_7 + y_i L_{11})Z_i + y_i + L_8 = 0 \quad \text{.... (12)}$$

Having computed the eleven unknowns coefficients (L_1 to L_{11}) for each one of the two photos, the object-space coordinates of any object point which is imaged in both photos can be computed using the above equations. So, if there is ground point A and its image appears in two photos, where a1 is the image of A in the left photo and a2 is the image of A in the right photo, two equations of the form (11 and 12) can be written for

point a1 and two more for point a2. This yields a system of four equations which contain only three unknown that are the ground coordinates of point A, (X,Y&Z). The values of X,Y&Z are computed in a L.S. solution. Depending upon this procedure the ground coordinates of matching points (TIN) are computed for later use.

2.2.4 Interpolation process

In this step, the elevation Z of the desired point must be interpolated from the surrounding data, and this is done by using the bilinear polynomial. The general form of this polynomial is ,**Ahmed, 1999**.

$$Z = a_0 + a_1 X + a_2 Y + a_3 XY \quad \ldots. (13)$$

Ground coordinates (X,Y & Z) of the matching points that have been computed in the previous section, are often called (as mentioned before) Triangulated Irregular Network (TIN). TIN is used here directly to find the elevation value (Z) for each pixel of the orthophoto, and this is done by interpolation process using multi-surfaces of bilinear polynomial equation Z=f(X,Y), for representing the study spot, depending on the ground coordinates of matching points.

The solution of this polynomial is by standard L.S. method. The calculated coefficients of the polynomial equations are used to find the elevation Z at each pixel ground (X,Y) of the orthophoto region. After that, these calculated ground coordinates (X,Y,Z) for each pixel in the orthophoto and the previously calculated parameters (L_1 to L_{11}) are used in the DLT Eqs. (1) and (2) to compute corresponding digital image coordinates directly then interpolate the gray value.

2.2.5 Resampling

One of the digital images (left image in our case) can now be transformed into an orthophoto. It is necessary to find the gray value for each pixel in the orthophoto as a final step, and this is done by interpolation the intensity levels for the new pixel locations from the neighboring old pixels using one of the following resampling methods, **Habib, 2004.** and **,Wolf & Dewitt, 2000.**

1. Nearest neighbor

Uses the value of the closest pixel to assign to the output pixel value.

2. Bilinear interpolation

Uses the data file values of four pixels in a 2*2 window to calculate an output value with bilinear function.

3. Cubic convolution

Uses the data file values of sixteen pixels in a 4*4 window to calculate an output value with a cubic function.

Cubic convolution interpolation is the best of these resampling methods, and for that reason we used this method in our case, applying the following equation in computing the gray value for each new pixel, (for understanding the equation below, seek for help using **Fig.**

$$g = g_{11}r_1c_1 + g_{12}r_1c_2 + g_{13}r_1c_3 + g_{14}r_1c_4 +$$
$$g_{21}r_2c_1 + g_{22}r_2c_2 + g_{23}r_2c_3 + g_{24}r_2c_4 +$$
$$g_{31}r_3c_1 + g_{32}r_3c_2 + g_{33}r_3c_3 + g_{34}r_3c_4 +$$
$$g_{41}r_4c_1 + g_{42}r_4c_2 + g_{43}r_4c_3 + g_{44}r_4c_4 \quad \ldots. (14)$$

Where:

g's are the intensity values of old pixels
r's are the rows
c's are the columns

The final orthophoto is represented in fig. 5

3. ACCURACY

The accuracy test was carried out in the middle of the processes of our final product, using 3 check points whose coordinates were determined with very high accuracy with terrestrial methods. After we compute the coordinates of these check points as mentioned in section (2.2.3) we compute the R.M.S.E. in 3-dimensions and the following deviations we obtained:

R.M.S.E. in X direction = 10.887 mm.
R.M.S.E. in Y direction = 8.302 mm.
R.M.S.E. in Z direction = 12.546 mm.

4. CONCLUSIONS

Carrying out comparative tests for the accuracy and functionality of the production procedures of digital orthophotos from aerial imagery established their usage in a wide range of applications. The use of orthophoto from close-range photos with high curved surfaces in architectural and archaeological applications has not been yet taken the range of hoping studies in investigate a lot of considerations that concerned with final accuracy to be achieved. I hope this paper be one of these papers that deals with some negligible cases in close-range photogrammetry and gained the hopeful results.

REFERENCES

- ,Ayman F. Habib, 2004. *Image registration & rectification*, Internet document,.
- ,C. loannidis, P. Pappa, S. Soile, E. Tsiliggiris and A. Georgopoulos, 2003, *Orthophoto Production Comparision Test for Close-Range Applications*.
- ,Edward M. Mikhail, James S. Bethel & J. Chris Mcglone, 2001, *Introduction to Modern Photogrammetry*, 1st edition.
- ,Maitham Mutasher Sharki, 2002, *Accuracy Assessment of Digital and Analytical Close-Range Photogrammetric Techniques*, MSc., Thesis, Baghdad University.
- ,Matthias Hemmleb, 2002, *Digital Rectification of Historical Images*, Internet document,.
- ,Paul R. Wolf and Bon A. Dewitt, 2000, *Elements of Photogrammetry with Applications in GIS*", 3rd edition,.
- ,Shaker Farhan Ahmed, 1999, *Automatic Production of Digital Orthophoto*, MSc. Thesis, Baghdad University.

+ control points
Θ check points

Figure 1. The target showing the position of 15 marked points.

Table 1. Ground control points for target points (field work).

Point	Type	X m.	Y m.	Z m.
1	check	501.924178	500.880956	51.259153
2	control	501.921455	500.862285	51.243883
3	control	501.945059	500.895585	51.247527
4	control	501.948533	500.866530	51.221669
5	control	501.949258	500.881047	51.226763
6	control	501.947706	500.885826	51.199257
7	control	501.944425	500.856190	51.181453
8	control	501.931662	500.851477	51.194789
9	control	501.943788	500.861170	51.172069
10	check	501.928334	500.856569	51.164549
11	check	501.949616	500.870282	51.152067
12	control	501.933537	500.862130	51.140041
13	control	501.920173	500.836603	51.119302
14	control	501.934250	500.885378	51.117134
15	control	501.920305	500.866149	51.103992

Table 2. Digital camera specifications.

Sensor	5.1 megapixel CMOS
Lens	F 2.8 ~ 8.47
Built-in view finder	Field of view: 85%
Focus range	Normal: 100cm ~ infinity Macro: (w) 20cm
Sensitivity	Auto , 100 , 200 , 400
LCD display	1.5" color TFT LCD panel
Still image resolution	2560 x 1920 , 2048 x 1536 , 1024 x 768
Still image quality	Fine: 7x compression rate Normal: 10x compression rate
Exposure control	Auto & manual
Shutter control	Mechanical shutter , shutter speed: 1/2 -1/6458 sec. with CCD variable electronic shutter
Digital zoom	4x
Image file format	JPEG compression
Picture storage	Internal: 16 MB embedded Nandgate flash memory External: SD memory card / MMC
Communication interface	USB 1.1
Power supply	AAA-size alkaline batteries x 4 Rechargeable Ni-MH batteries (min.550mAh/1.2V)
Dimensions	Camera body: 97 x 28 x 63 mm
Weight	Camera body without battery: 110 g

Left photo **Right photo**

Figure 2. The left and right photos for the target.

Table 3. Digital coordinates of ground control points.

Point	Left Photo		Right Photo	
	column	row	column	row
1	1362.67	418.67	1102.00	492.00
2	1398.00	508.67	1172.67	566.00
3	1226.00	484.00	1009.33	564.00
4	1292.67	620.00	1115.33	678.67
5	1230.67	591.33	1047.33	659.33
6	1266.00	721.33	1036.67	778.67
7	1328.00	807.33	1152.67	857.33
8	1396.67	747.33	1219.33	792.00
9	1307.33	856.67	1121.33	902.67
10	1413.33	876.67	1200.00	916.67
11	1285.33	955.33	1079.33	992.00
12	1364.00	1008.00	1136.00	1042.67
13	1451.33	1084.00	1256.00	1132.67
14	1297.33	1128.00	1032.67	1151.33
15	1414.00	1179.33	1145.33	1206.67

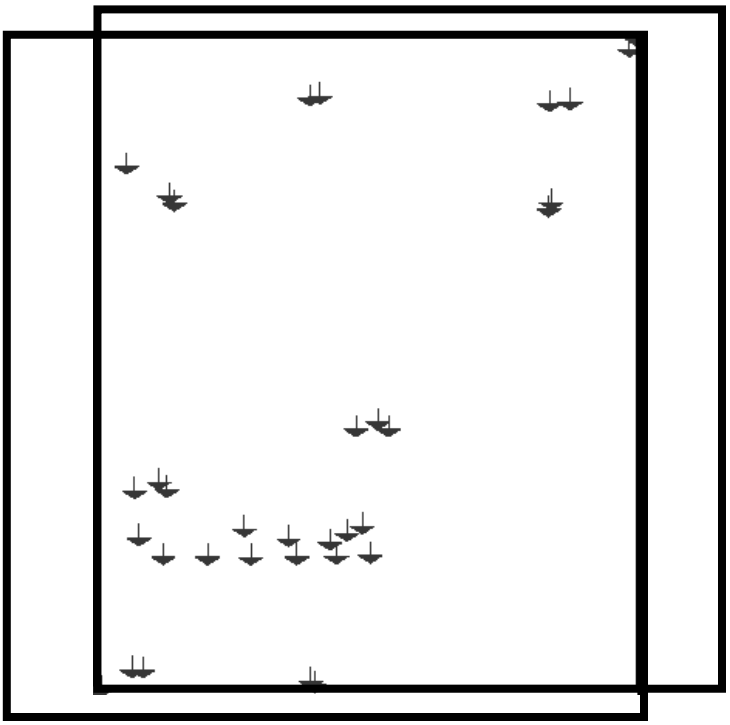

Figure 3. The distribution of matching points on the target.

Table 4. Digital coordinates of matched points.

Point	Left Photo		Right Photo	
	column	row	column	row
1	1182.00	102.67	1028.00	223.33
2	1188.00	102.00	1030.00	210.00
3	1346.00	113.33	1163.33	193.33
4	1343.33	121.33	1172.00	196.00
5	1210.67	151.33	1150.67	242.67
6	1218.67	150.67	1156.67	241.33
7	1357.33	482.00	1104.67	550.67
8	1326.67	491.33	1076.00	564.00
9	1370.00	505.33	1128.67	570.00
10	1294.00	517.33	1058.00	590.00
11	1381.33	524.00	1154.00	587.33
12	1216.00	493.33	1001.33	574.67
13	1212.67	615.33	1028.67	682.67
14	1236.67	618.67	1050.00	685.33
15	1230.67	638.67	1036.00	704.00
16	1376.67	776.00	1198.00	820.00
17	1400.67	776.33	1217.33	820.67
18	1392.67	794.67	1201.33	838.00
19	1206.67	1457.33	880.00	1438.67
20	1238.67	1380.67	919.33	1373.33
21	1242.00	1361.33	922.00	1357.33
22	1521.33	1364.00	1176.00	1384.00
23	1519.33	1346.67	1174.67	1368.67
24	1342.67	1634.00	919.33	1610.00
25	1350.00	1639.33	906.67	1613.33
26	1520.00	1619.33	1080.00	1621.33
27	1535.33	1624.00	1071.33	1627.33
28	1579.33	1761.33	1117.33	1763.33
29	1584.67	1788.67	1120.00	1791.33
30	1362.00	446.00	1104.00	519.33
31	1332.67	444.00	1075.33	520.67
32	1298.67	443.33	1046.00	524.00
33	1266.67	444.00	1024.00	526.00
34	1234.00	444.67	1007.33	528.67
35	1387.33	448.67	1136.67	518.67

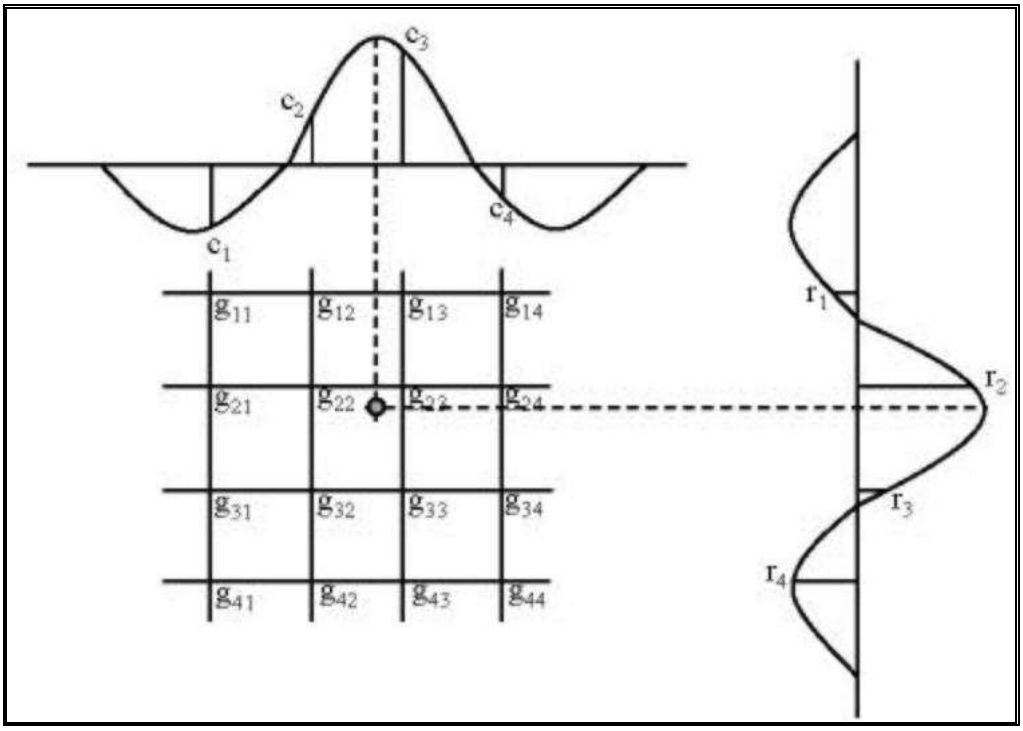

Figure 4. Bicubic convolution.

Figure 5. Digital orthophoto of case study.